Effect of power history on pellet-cladding interaction

Kisik Hong[a], J.R. Barber[a], M.D. Thouless[a,b], Wei Lu[a,b,*]

[a] Department of Mechanical Engineering, University of Michigan, Ann Arbor, Michigan 48109

[b] Department of Materials Science & Engineering, University of Michigan, Ann Arbor, Michigan 48109

Abstract

In this paper, the mechanical pellet-cladding interaction (PCI) is studied under various power histories. We find that the power history significantly affects possible PCI failure. PCI during the thermal transient period of power ramping occurs in such a way that crack-mouth opening increases regardless of when contact is initiated, before or during power ramping. The crack-mouth opening continues to increase further during the thermal steady state (during the power ramp). Conversely, PCI initiated either during the thermal steady-state power ramp or during the normal operation (with no power ramp) leads to decrease in crack-mouth opening. As a consequence, PCI initiated before power ramping or during the transient period of power ramping leads to high local tensile hoop stress. In contrast, PCI initiated during the thermal steady state of power ramping or during the normal operation without power ramping leads to local compressive hoop stress. In the former case, PCI failure near the crack tip might be anticipated (by either brittle failure during the transient power ramp or failure during the steady-state power ramp), whereas in the latter case, it is suppressed.

*Corresponding author

E-mail address: weilu@umich.edu

1. Introduction

Upon the initial start-up of light-water reactors, large thermal gradients are generated within the fuel pellets owing to the low thermal conductivity of UO_2. These gradients induce tensile hoop stresses at the outer surface of the pellet, which lead to fuel fragmentation (Oguma, 1983). As the cladding creeps down, and the fuel swells, contact between the fuel and cladding eventually occurs. The interaction between the crack edges in the pellet and the cladding introduces local singular stresses within the cladding. These local singular stresses can lead to cladding failure, which is occasionally observed during operation with significant power uprating (Cox, 1990; Penn *et al.*, 1977).

Several studies have investigated the interaction between the pellet and cladding, often termed pellet-cladding interaction (PCI). These include analytical studies conducted to predict the stress distribution (Gittus, 1972; Roberts *et al.*, 1977), and experimental studies to mimic PCI and to evaluate attributes associated with resistance to failure from PCI (Rosenbaum *et al.*, 1987; Wood *et al.*, 1975). Recently, finite-element simulations that incorporate various complex mechanisms, such as creep, fuel swelling, and thermal expansion have been performed to provide insight into how PCI can induce failure (Marchal *et al.*, 2009; Michel *et al.*, 2013, 2008; Sercombe *et al.*, 2012). This recent work focused on a very specific loading scenario. However, since the phenomena involved in the PCI problem have distinct time-scales, and since frictional contact problems are inherently history-dependent, different loading histories can lead to very divergent results. Our interest in this paper is to distinguish the types of power history that can lead to failure from PCI from the types of power history that can lead to more benign forms of PCI. We do this by modeling the evolution of hoop stresses at the inner surface of the cladding under different loading scenarios, using detailed finite-element calculations, as described below.

2. Finite-element model

2.1 Geometry and boundary conditions

A finite-element model for a fuel rod was constructed as shown in Fig. 1, where the dimensions were defined at 300 K. This 2-D plane-strain model representing the middle cross-sectional plane of a fuel rod, which includes the UO_2 fuel pellet and Zircaloy cladding, was implemented using the commercial software ABAQUS. A 3-D model of the fuel rod might be ideal to capture the details of PCI, since a 2-D model does not, for example, account for the hourglass shape of pellet. However, a 2-D model can reasonably explain the interaction between the cracked fuel and cladding with a refined mesh at a relatively low computational cost.

Since experimental observations indicate that fuel pellets are fragmented into pieces during the initial start-up, with the number of pieces depending on the power level (Oguma, 1983), we considered the case where there are 8 pieces. Therefore, we model half of a fragmented piece (so the angle in Fig. 1 is 22.5°) with symmetric boundary conditions. The cracked surface of the pellet $\theta = 0°$ is also a symmetry plane, and the boundary conditions there are equivalent to a frictionless hard contact with a rigid surface.

The gauge pressure on the outside of the cladding was assumed to be 12 MPa, representing the difference between the external coolant pressure and the internal helium pressure (Johnson *et al.*, 1982). A hard-contact condition was used at the interface between the pellet and cladding to ensure no penetration. A Coulomb friction law was implemented at this contact using the Lagrange-multiplier method. The coefficient of friction between the pellet and cladding was set to be 0.7 (Wood *et al.*, 1980). The initial temperature of the fuel rod was set to be 300 K, but then allowed to heat up as power is generated within the fuel. The temperature of

the outer surface of the cladding was set to 600 K, which is equivalent to the temperature of the primary coolant.

2.2 Mechanisms

The creep law for Zircaloy was taken from the deformation-mechanism map of Wang *et al*. (Wang *et al.*, 2013), while that for UO_2 was taken from the deformation-mechanism map of Frost and Ashby (Frost and Ashby, 1982). Grain sizes, which affect creep, were assumed to be 50 μm for Zircaloy and 10 μm for UO_2. The swelling of UO_2, resulting from the accumulation of solid and gaseous fission products, was implemented using the MATPRO model (Siefken *et al.*, 2001). The fuel expansion due to swelling can be partially offset during early irradiation by fuel densification induced by irradiation sintering. We therefore implemented the model from MATPRO (Siefken et al., 2001) to incorporate fuel densification. The amount of densification depends on the initial porosity of the fuel (Energy, 1993). Other material parameters for the Zircaloy, UO_2, and helium were also taken from MATPRO (Siefken *et al.*, 2001).

2.3 Mesh refinement

We used first-order, coupled temperature-displacement, plane-strain elements with reduced integration for implicit calculations. Refined meshes were used near the corner of the cracked pellet and near the cladding inner surface at $\theta = 0°$ to capture any stress singularities near the contact between the cracked pellet and cladding. We confirmed that the mesh was fine enough by comparing the strength of singularity calculated from a finite-element simulation with analytical solutions for the geometry. Since creep relaxation causes the singularity to decrease with time, this validation was made for the case at T = 600 K, with no creep and a non-slip interface, resulting in an elastic singularity. The strength of this singularity was obtained by calculating the slope of the log-log plot of stress against the distance from the contact point along

the inner surface of the cladding. The singularity from the finite-element calculation, 0.509±0.0005, agreed well with the analytical value of 0.5093 (Bogy, 1971).

3. Results and discussion

The output of a nuclear power station is adjusted according to demand by the insertion of control rods into the reactor. If there is an increase in demand, the power level increases during what is known as power ramping. This leads to three possible power histories for which we consider the effects of PCI: (i) power ramping after contact has already been established between the cladding and fuel, (ii) power ramping before contact has been established, and (iii) normal operation with no power ramping. In the models presented below, the last scenario is considered as part of the first, so it is not addressed specifically in a separate section. Note that the return to normal operation after a power ramp is specifically considered in our study.

3.1 Power ramping after contact

We implemented a power history based on a typical experimental protocol of power ramp tests, similar to that used for the TRANS-RAMP project (Mogard and Kjaer-Pedersen, 1985), where a power ramp is established after a pre-conditioning period at nominal power (Cox, 1990). The power history modelled in this section consists of eighteen months under normal conditions, followed by a month-long power ramp before returning to normal conditions. The thermal power generated per unit length of the fuel rod (linear heat rate (LHR) of the fuel) was assumed to be uniform and equal to 20 kW/m during normal operation, and 40 kW/m during the power ramp. The transitions between normal operation and the power ramp were assumed to occur as a step change in the power generation, reflecting the relatively rapid ramp rate used for the power ramp tests (Cox, 1990). However, we also considered the case with a ramp rate of 10 kW/m·min, instead of a step change. These calculations showed that a finite time-scale of the power transient

has a negligible effect on the result, especially in terms of interaction between the cracked fuel and cladding, since the time-scale of heat transfer is relatively small compared to that of other mechanisms.

3.1.1 Opening of radial cracks within the pellet

Contact between the fragmented pellet (with a sharp corner at the crack mouth) and the cladding results in a singular stress field at the inner surface of the cladding. Since the direction of relative slip between the pellet and cladding determines the sign of the singular hoop stress, we tracked the crack-mouth opening of the radial crack in the pellet. This is shown in Fig. 2a, along with the corresponding gap between the pellet and cladding.

Upon start-up, the temperature within the pellet increases instantaneously and a large temperature gradient is established within the pellet. This temperature gradient leads to an immediate increase in the crack-mouth opening. (It should be noted that a uniform temperature increase (or a uniform swelling) expansion will not open up initially closed cracks). As the gap between the pellet and cladding decreases with time, owing to fuel swelling and creep-down of the cladding, the heat-transfer associated with the helium-filled gap increases. In addition, the thermal conductivity of UO_2 increases with decreasing temperature (Siefken *et al.*, 2001), so both the temperature and temperature gradient within the pellet are reduced after reaching a maximum 50 s after start-up, as shown in Fig. 3. These effects lead to a slight decrease in the crack-mouth opening before contact occurs at about 25 months, as shown in Fig. 2a.

After contact occurs, the system reaches a new thermal steady state within a minute. Although we anticipate some residual thermal contact resistance owing to the roughness of contacting surfaces after the gap closes (Cooper and Yovanovich, 1969), it is much lower than

the thermal resistance of the helium-filled gap and is therefore neglected. We also note that this assumption makes the contact resistance change continuously between separation and contact, which ensures that the coupled thermoelastic contact problem is mathematically well-posed and stable (Barber *et al.*, 1980). While in contact with the cladding, the fuel swelling in radial direction is less than it would have been without contact. The contact pressure then causes lateral expansion, resulting in a decrease in the crack-mouth opening as shown in Fig. 2a. Though the decrease is not significant, we should note that it determines the sign of the singular stress near the contact with the crack mouth, which will be discussed in the following section.

Power ramping leads to rapid increases in both the temperature of the fuel pellet and the temperature gradient within it; this causes the crack to open up significantly during the period of the thermal transient period (within a minute), as shown in Fig. 2b. In addition, the thermal expansion of the pellet induces a high contact stress, which leads to enhanced creep of the cladding. As a result, the crack continues to open with time, even after the system reaches a thermal steady state; this can be seen within the power-ramping region of Fig. 2a.

During the period of increased power generation, the rate of fuel swelling increases, causing the cladding to creep outwards while in contact with the pellet. When the power decreases to its original level after power ramping, the thermal strains generated during the power ramp disappear; however, the permanent deformation associated with the creep and the swelling of the fuel remain. As a consequence, the pellet and cladding lose contact immediately after the return to normal operating conditions, and the crack opening decreases (see the right end of Fig. 2a). As the normal operating conditions continue, contact eventually occurs again owing to swelling of the fuel and creep-down of the cladding, the local hoop stress at the inner surface of the cladding near the crack edge is compressive until another power ramp occurs.

With a second power ramp of the same magnitude, the crack-mouth opening increases again to a value similar to that during the previous power ramp.

During operation, the temperature increase of the helium gas, and the release of fission gases from the fuel, can increase the internal pressure within the fuel rod (Williamson et al., 2012). Calculations using an increased helium pressure of 16 MPa showed that this leads to a delayed onset of PCI, owing to the reduced rate of cladding creep-down. Fuel densification also delays the initiation of PCI. However, neither of these phenomena affects the sign of the local singular hoop stress induced by the interaction between the cracked fuel and cladding.

3.1.2 Evolution of the hoop stress at the inner surface of the cladding

Figure 4 shows the hoop stresses at the inner surface of the cladding at different times during normal operation after contact occurs. The deformation of the pellet associated with the presence of the crack leads to a gradual contact along the inner surface of the cladding. The contact is initiated next to the crack mouth (Fig. 4a); it then occurs near the center of the fuel fragment (Fig. 4c), and, finally, the two regions meet up (Fig. 4d). The far-field hoop stress away from the crack edge, increases owing to the fuel swelling. Since this sharp corner slips relative to the cladding in a direction that reduces the crack-mouth opening, the local hoop stresses are singular and compressive.

When power ramping occurs, the thermal expansion of the pellet greatly increases the hoop stress in the cladding, as the pellet pushes the cladding radially outward, as in Fig. 5a. Note that the far-field hoop stress is not uniform along the cladding surface because the opening crack induces a non-uniform contact pressure on the inner surface of the cladding. The local hoop stress at the inner surface of the cladding in the vicinity of the crack mouth becomes tensile

(positive) immediately after power ramping is established. It is associated with the opening of the crack owing to an increase in the thermal gradient within pellet, which agrees with previous simulation results (Marchal *et al*., 2009; Michel *et al.*, 2013, 2008; Sercombe *et al*., 2012).

The far-field hoop stress relaxes with time, as shown by the plots of the hoop-stress distribution at different times in Fig. 5. This arises because the outward creep of the cladding relaxes the hoop stress more than the fuel swelling increases it. Also, both the strengths of the singularities for the hoop stresses and their magnitude decrease with time, owing to creep of the cladding.

During the transient period of power ramping, the deformation of the cladding is predominantly elastic, and the creep zone (the region where the creep strain exceeds the elastic strain) is confined to a very small region at the crack tip. However, the creep zone grows larger during steady-state power generation. Therefore, brittle failure might be anticipated during the transient period, whereas failure during the steady state is more likely to be associated with creep.

3.2 Power ramping before contact

If power ramping occurs before contact occurs during normal operation, PCI may be initiated either during the initial thermal transient period of the power ramp, or after the system reaches the thermal steady state of the power ramp, depending on the gap at the time when the power is ramped. We will investigate both cases in the following sections.

3.2.1 Contact occurring during the thermal transient of a power ramp

We first consider the case where contact is established during the thermal transient associated with power ramping. To model this scenario, we assumed that the fuel rod is

subjected to eighteen months of normal operation (LHR = 20 kW/m), followed by a power ramp (LHR = 40 kW/m) for one month, and then continued operation at a normal level.

Under the conditions described above, contact first occurs during the transient period of power ramping (Fig. 6a). In contrast to the previous case where contact spreads with time along the inner surface of the cladding, contact occurs almost immediately (within a minute) after the onset of the power ramp as a result of rapid thermal expansion of the fuel pellet (Fig. 6b). In addition, an increased thermal gradient within the pellet causes the crack to open. This continues after contact occurs at a reduced rate owing to frictional interaction with the cladding. After the system reaches a thermal steady state, the crack-mouth opening continues to increase, as the cladding creeps radially outward (see section 3.1.1).

After a return to normal operation, the gap between the pellet and cladding again opens up owing to the thermal contraction of the pellet (Fig. 6a). The gap after the power ramp is smaller than it was before the power ramp because fuel swelling, which reduces the gap, dominates over creep of the cladding, which increases the gap. The crack-mouth opening decreases when normal operating conditions are restored owing to the decreased thermal gradient in the pellet (see section 3.1).

Figure 7 shows the evolution of the hoop stress at the inner surface of the cladding after contact occurs. Since the crack keeps on opening, the local hoop stress is tensile. The result is qualitatively similar to that described for the previous scenario (section 3.1 and Fig. 5).

3.2.2 Contact occurring during thermal steady state of a power ramp

We finally consider the case where PCI is initiated during the thermal steady state of a power ramp. For PCI not to occur during the transient period, the gap at the instant of power

ramping needs to be large enough, as would be the case if the power ramp occurs very early during operation, such as 9 months after the initial start-up.

Figure 8a shows that while a power ramp may not be big enough to close the gap between the pellet and cladding, it does causes a large decrease in the gap within a few seconds (Fig. 8b). The gap is subsequently closed by further swelling of the fuel and by the increased creep rate of the cladding associated with the higher temperatures of a power ramp. After contact, the crack closes because of the fuel swelling. After normal operating conditions are restored, the gap between the pellet and cladding opens up again, and the crack closes, as before (section 3.1.1).

In this case, the local hoop stress remains compressive, regardless of the dwell time (Fig. 9). We note that the result is qualitatively similar to that of the previous scenario (section 3.1 and Fig. 4). The local compressive hoop stresses helps to suppress PCI failure. Therefore, if failure occurs under this condition, it is possible only in regions away from the crack, and is caused by the far-field tensile hoop stress induced by fuel swelling.

This scenario can also be obtained by reducing the increase in power level, which we confirmed by a separate calculation with a 20% increase during the power ramping. The results show that power ramping can possibly be achieved without causing local tensile hoop stresses associated with PCI failure, if contact occurs after the system has evolved to the thermal steady state. The above results could explain the experimental observation (Mogard and Kjaer-Pedersen, 1985) that there exists a power-level threshold below which the fuel may be ramped without resulting in PCI failure (Cox, 1990).

4. Conclusions

We have investigated conditions at which PCI failure may occur by considering some representative power histories. The results can give an insight into developing safety criteria for operation of reactors. Finite-element models have been developed to study the evolution of the hoop stresses at the inner surface of the cladding for different power histories. The power history significantly affects possible PCI failure. It has been found that the local stresses in the vicinity of the crack can be tensile or compressive depending on when contact between the cladding and pellet occurs. During the thermal transient period of a power ramp, PCI occurs in such a way that the crack-mouth opens up in response to the increased temperature gradient within the pellet. The crack continues to open further, even after the system reaches a thermal steady state (during the power ramp), owing to enhanced creep of the cladding. The result is valid regardless of when contact is initiated, before or during power ramping. However, PCI initiated during the thermal steady state for either a power ramp or normal operation leads to crack opening decrease controlled by fuel swelling.

Based on results of this paper, we can conclude that high local tensile hoop stresses are induced if an interaction between the pellet and cladding is initiated either before power ramping or during the transient period of a power ramps. Conversely, local compressive hoop stresses are induced if the interaction is during the steady state portions of normal operation or a power ramp. Therefore, PCI failure near the crack tip might be anticipated (by either brittle failure during the transient power ramp or failure during the steady-state power ramp) in the former case, while it is expected to be suppressed in the latter case.

Acknowledgements

This research was supported by the Consortium for Advanced Simulation of Light Water Reactors (http://www.casl.gov), an Energy Innovation Hub (http://www.energy.gov/hubs) for Modeling and Simulation of Nuclear Reactors under U.S. Department of Energy Contract No. DE-AC05-00OR22725.

References

Barber, J.R., Dundurs, J., Comninou, M., 1980. Stability considerations in thermoelastic contact. J. Appl. Mech. 47, 871–874.

Bogy, D., 1971. Two edge-bonded elastic wedges of different materials and wedge angles under surface tractions. J. Appl. Mech. 38, 377–386.

Cooper, M.G., Yovanovich, B.B.M. and M.M., 1969. Thermal Contact Conductance. Int J. Heat Mass Transf. 12, 279–300.

Cox, B., 1990. Pellet-clad interaction (PCI) failures of zirconium alloy fuel cladding—a review. J. Nucl. Mater. 172, 249–292.

DOE Fundamentals Handbook: Material Science. U. S. Dep. Energy, 1993.

Frost, H.J., Ashby, M.F., 1982. Deformation mechanism maps: the plasticity and creep of metals and ceramics. Pergamon Press.

Gittus, J.H., 1972. Theoretical analysis of the strains produced in nuclear fuel cladding tubes by the expansion of cracked cylindrical fuel pellets. Nucl. Eng. Des. 18, 69–82.

Johnson, A.B., Gilbert, E.R., Guenther, R.J., 1982. Behavior of spent nuclear fuel and storage system components in dry interim storage. PNL-4189, Prep. U. S. Dep. Energy under Contract DE-AC06-76RLO 1830, Pacific Northwest Lab.

Marchal, N., Campos, C., Garnier, C., 2009. Finite element simulation of Pellet-Cladding Interaction (PCI) in nuclear fuel rods. Comput. Mater. Sci. 45, 821–826.

Michel, B., Nonon, C., Sercombe, J., Michel, F., Marelle, V., Nonon, C., Sercombe, J., Michel, F., Simulation, V.M., 2013. Simulation of pellet-cladding interaction with the pleiades fuel performance software environment. Nucl. Technol. 182, 124–137.

Michel, B., Sercombe, J., Thouvenin, G., Chatelet, R., 2008. 3D fuel cracking modelling in pellet cladding mechanical interaction. Eng. Fract. Mech. 75, 3581–3598.

Mogard, H., Kjaer-Pedersen, N., 1985. A review of Studsvik's international power ramp test projects. Studsvik AB Atomenergi. Rep. Studsvik-85/6.

Oguma, M., 1983. Cracking and relocation behavior of nuclear fuel pellets during rise to power. Nucl. Eng. Des. 76, 35–45.

Penn, W.J., Lo, R.K., Wood, J.C., 1977. CANDU fuel – power ramp performance criteria. Nucl. Technol. 34, 249–268.

Roberts, J.T.A., Smith, E., Fuhrman, N., Cubicciotti, D., 1977. On the pellet-cladding interaction phenomenon. Nucl. Technol. 35, 131–144.

Rosenbaum, H.S., Rand, R.A., Tucker, R.P., Cheng, B., Adamson, R.B., Davies, J.H., Armijo, J.S., Wisner, S.B., 1987. Zirconium-barrier cladding attributes. Zircon. Nucl. Ind. ASTM Int.

Sercombe, J., Aubrun, I., Nonon, C., 2012. Power ramped cladding stresses and strains in 3D simulations with burnup-dependent pellet–clad friction. Nucl. Eng. Des. 242, 164–181.

Siefken, L.J., Coryell, E.W., Harvego, E.A., Hohorst, J.K., 2001. SCDAP/RELAP5/MOD 3.3 Code Manual: MATPRO—A Library of Materials Properties for Light-Water-Reactor Accident Analysis. Idaho Natl. Eng. Environ. Lab.

Wang, H., Hu, Z., Lu, W., Thouless, M.D., 2013. A mechanism-based framework for the numerical analysis of creep in zircaloy-4. J. Nucl. Mater. 433, 188–198.

Williamson, R.L., Hales, J.D., Novascone, S.R., Tonks, M.R., Gaston, D.R., Permann, C.J., Andrs, D., Martineau, R.C., 2012. Multidimensional multiphysics simulation of nuclear fuel behavior. J. Nucl. Mater. 423, 149–163.

Wood, J.C., Surette, B.A., Aitchison, I., Clendening, W.R., 1980. Pellet cladding interaction—evaluation of lubrication by graphite. J. Nucl. Mater. 88, 81–94.
Wood, J.C., Surette, B.A., London, I.M., Barid, J., 1975. Environmentally induced fracture of zircaloy by iodine and cesium: the effects of strain rate, localized stresses and temperature. J. Nucl. Mater. 57, 155–179.

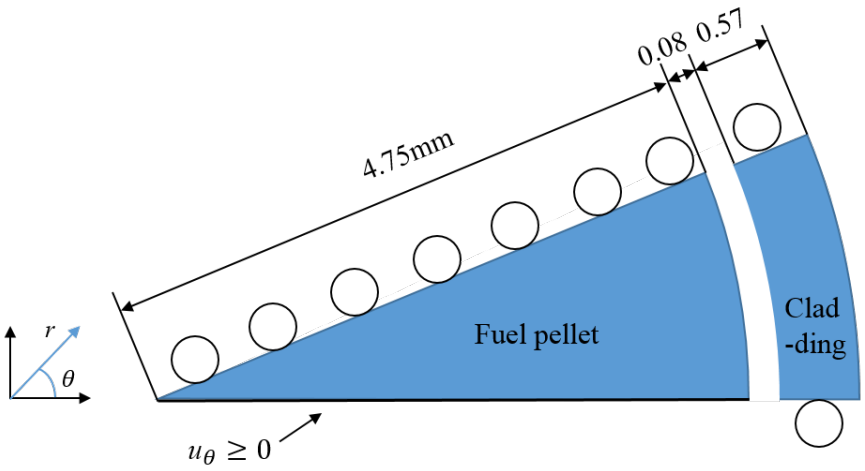

Figure 1: The fuel pellet was assumed to be fragmented into 8 pieces. 22.5° of the fuel assembly was modeled. A symmetrical boundary condition was applied along the $\theta = 22.5°$ plane within the fuel. A contact boundary was applied along the $\theta = 0°$ plane in the fuel (a crack plane). Thermal stresses held the crack surfaces together near the center of the pellet. Symmetry boundary conditions were applied at both $\theta = 0°$ and $\theta = 22.5°$ for the cladding.

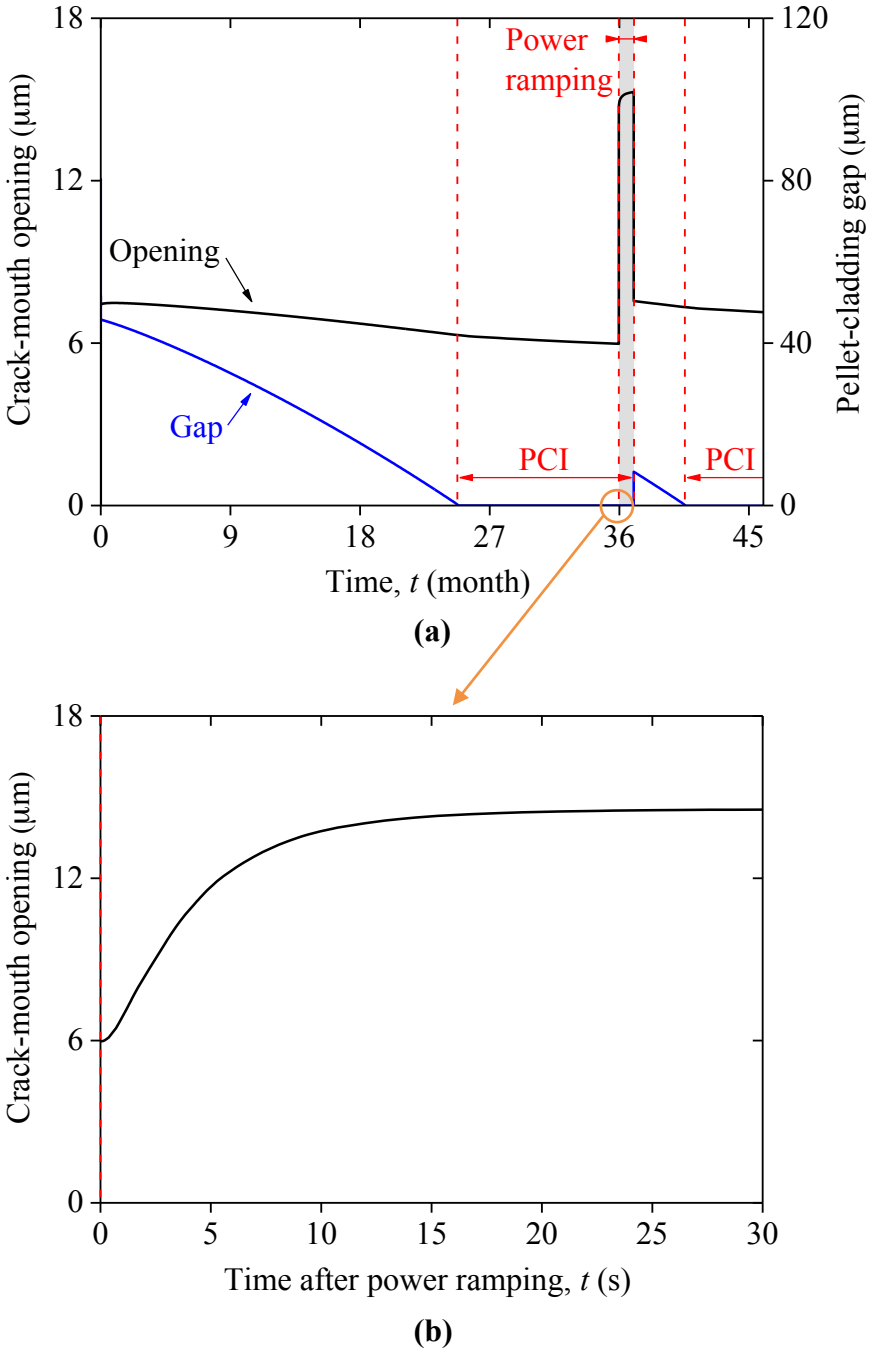

Figure 2: **(a)** The opening of the crack-mouth as a function of time for a cycle consisting of normal operation (LHR = 20 kW/m) for 36 months, a power ramp (LHR = 40 kW/m) for 1 month, and a return to normal operation. The shaded region shows power ramping. **(b)** A plot of crack-mouth opening as a function of time immediately after the beginning of the power ramp.

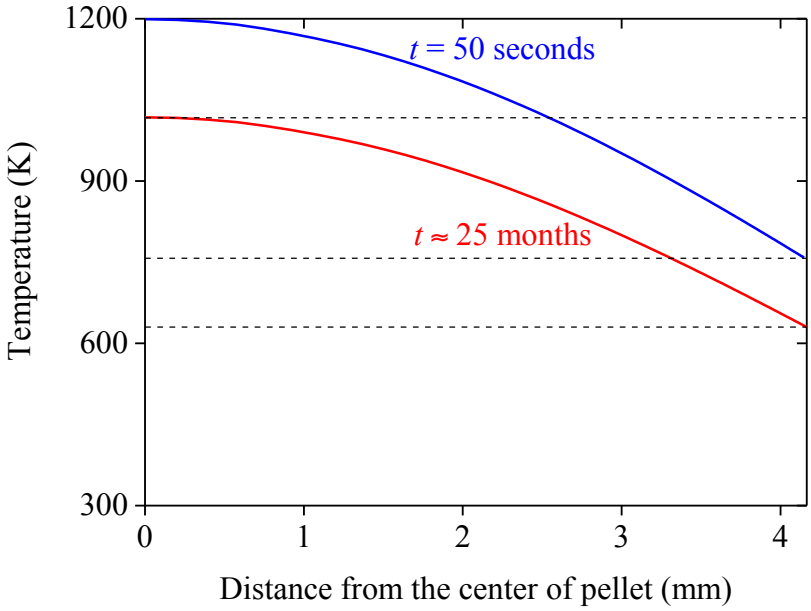

Figure 3: Radial temperature distribution for the pellet at different times, t, after the fuel rod is put into service. The temperature reaches a maximum at t = 50 seconds and decreases until contact occurs at $t \approx 25$ months.

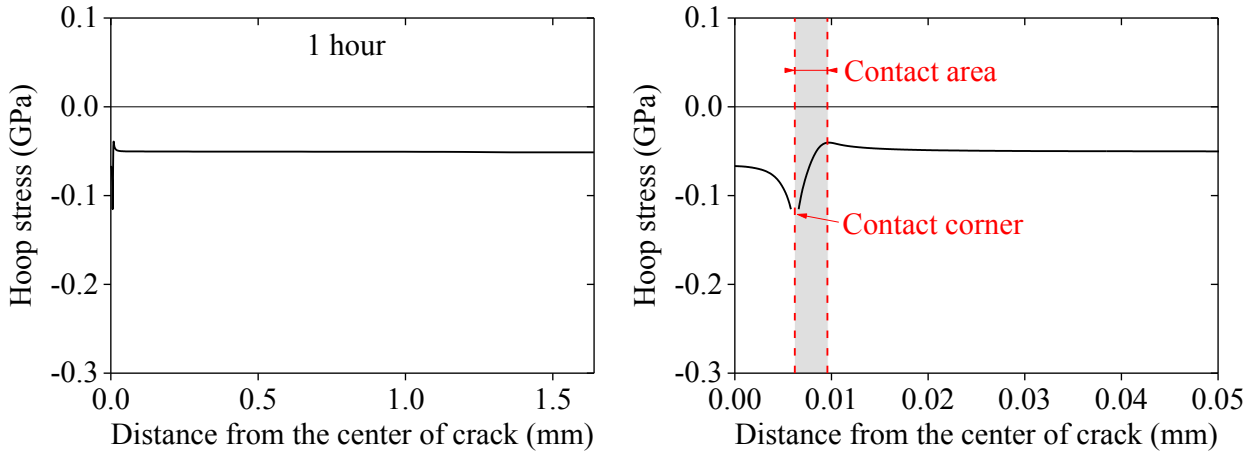
1 hour
Contact area
Contact corner
Hoop stress (GPa)
Distance from the center of crack (mm)
0.1
0.0
-0.1
-0.2
-0.3
0.0
0.5
1.0
1.5
0.00
0.01
0.02
0.03
0.04
0.05

(a)

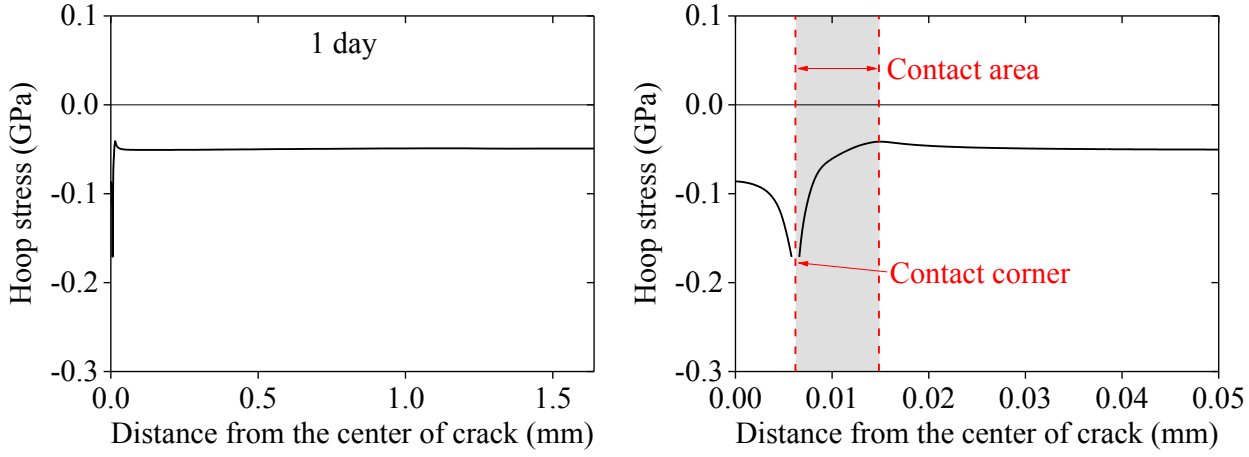
1 day
Contact area
Contact corner
Hoop stress (GPa)
Distance from the center of crack (mm)
0.1
0.0
-0.1
-0.2
-0.3
0.0
0.5
1.0
1.5
0.00
0.01
0.02
0.03
0.04
0.05

(b)

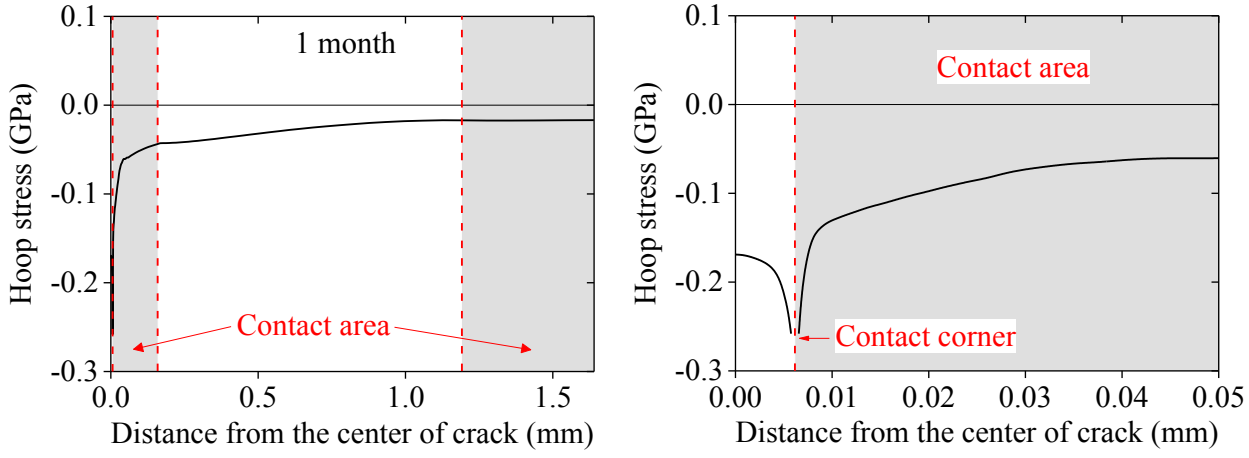
1 month
Contact area
Contact area
Contact corner
Hoop stress (GPa)
Distance from the center of crack (mm)
0.1
0.0
-0.1
-0.2
-0.3
0.0
0.5
1.0
1.5
0.00
0.01
0.02
0.03
0.04
0.05

(c)

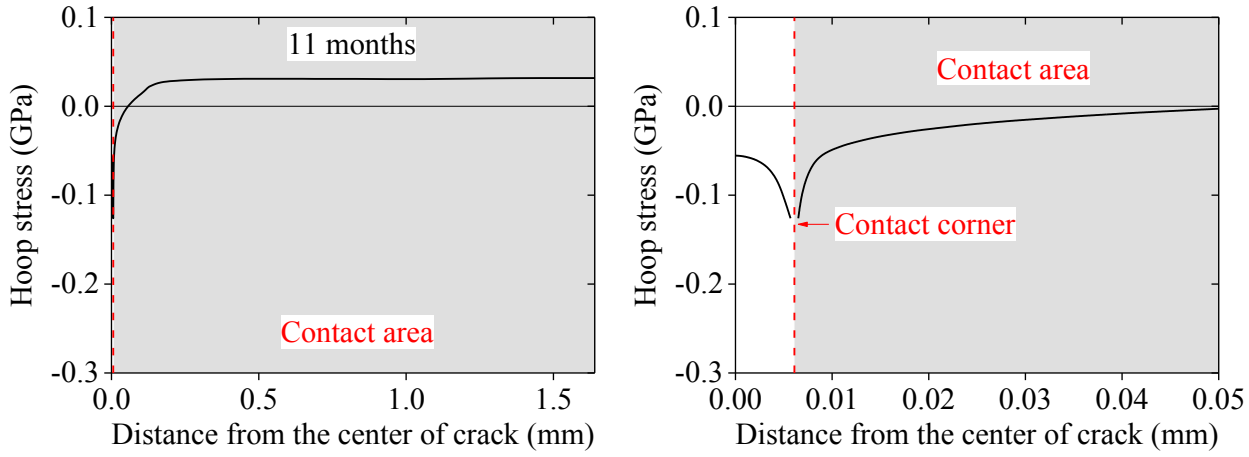

(d)

Figure 4: The distribution of the hoop stress at the inner surface of the cladding at different times after contact occurs under normal operating conditions. The figures to the right show details near the edge of the contact with the crack mouth. These figures correspond to **(a)** 1 hour, **(b)** 1 day, **(c)** 1 month, and **(d)** 11 months (immediately before the onset of the power ramp). The stresses at the edge of the crack are singular, as expected for contact with a creeping solid, so the stresses are shown as being discontinuous in that region.

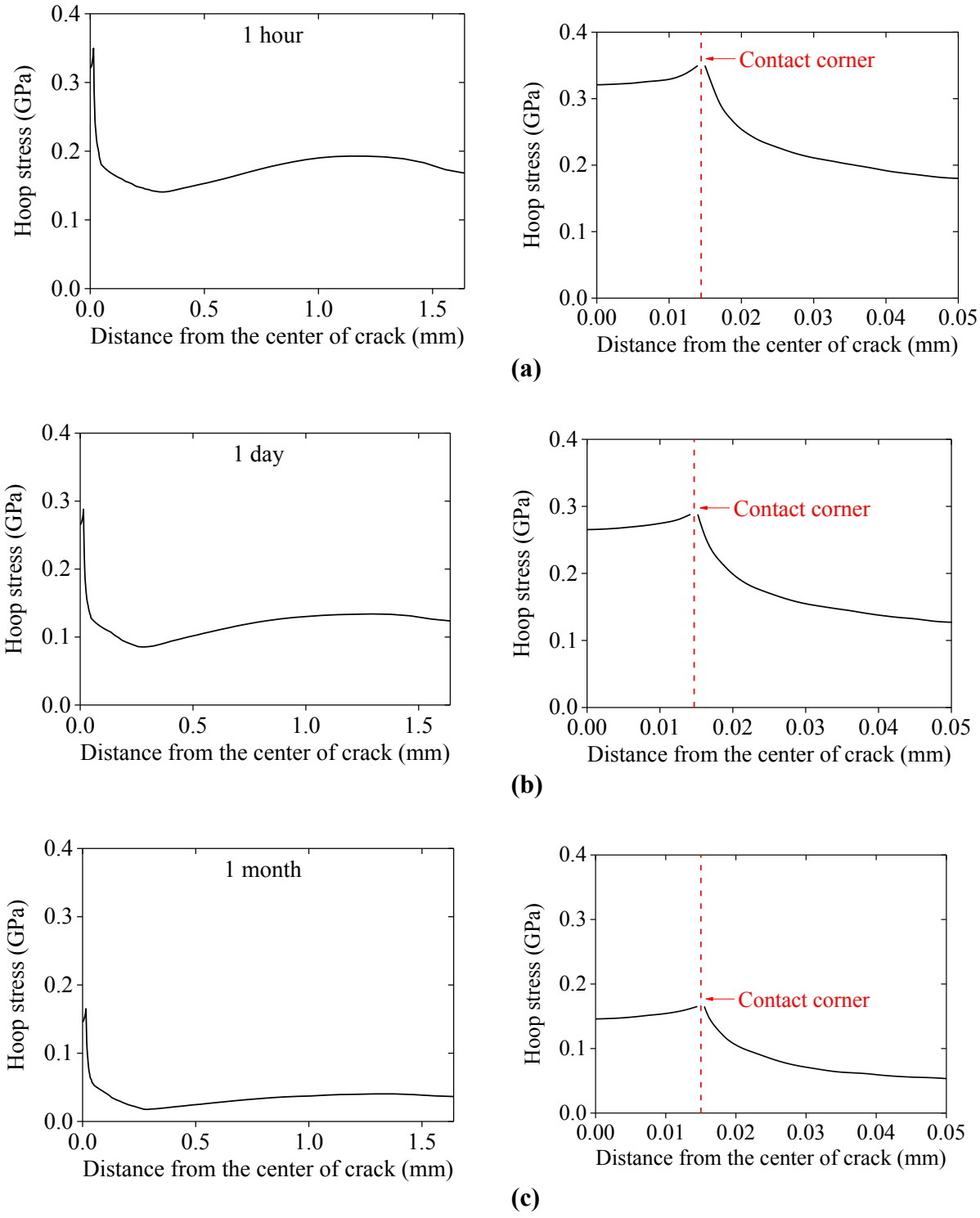

Figure 5: The distribution of hoop stresses at the inner surface of the cladding at **(a)** 1 hour, **(b)** 1 day, and **(c)** 1 month after the onset of a power ramp, with the power history of Fig. 2. The figures on the right show details near the crack mouth.

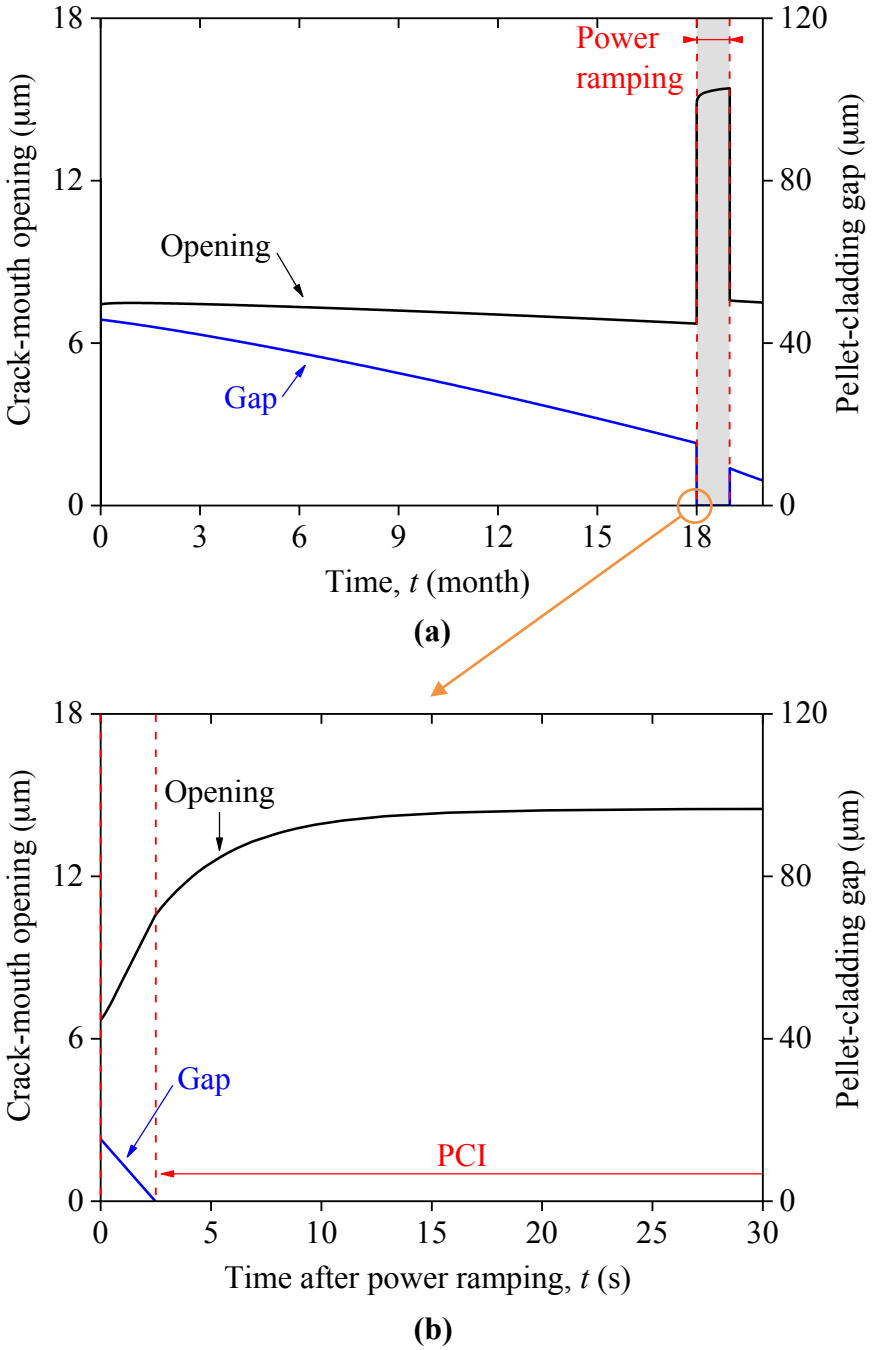

Figure 6: **(a)** The opening of the crack-mouth as a function of time for a cycle consisting of normal operation (LHR = 20 kW/m) for 18 months, a power ramp (LHR = 40 kW/m) for 1 month, and a return to normal operation. The shaded region shows power ramping. **(b)** A plot of crack-mouth opening as a function of time immediately after the beginning of the power ramp.

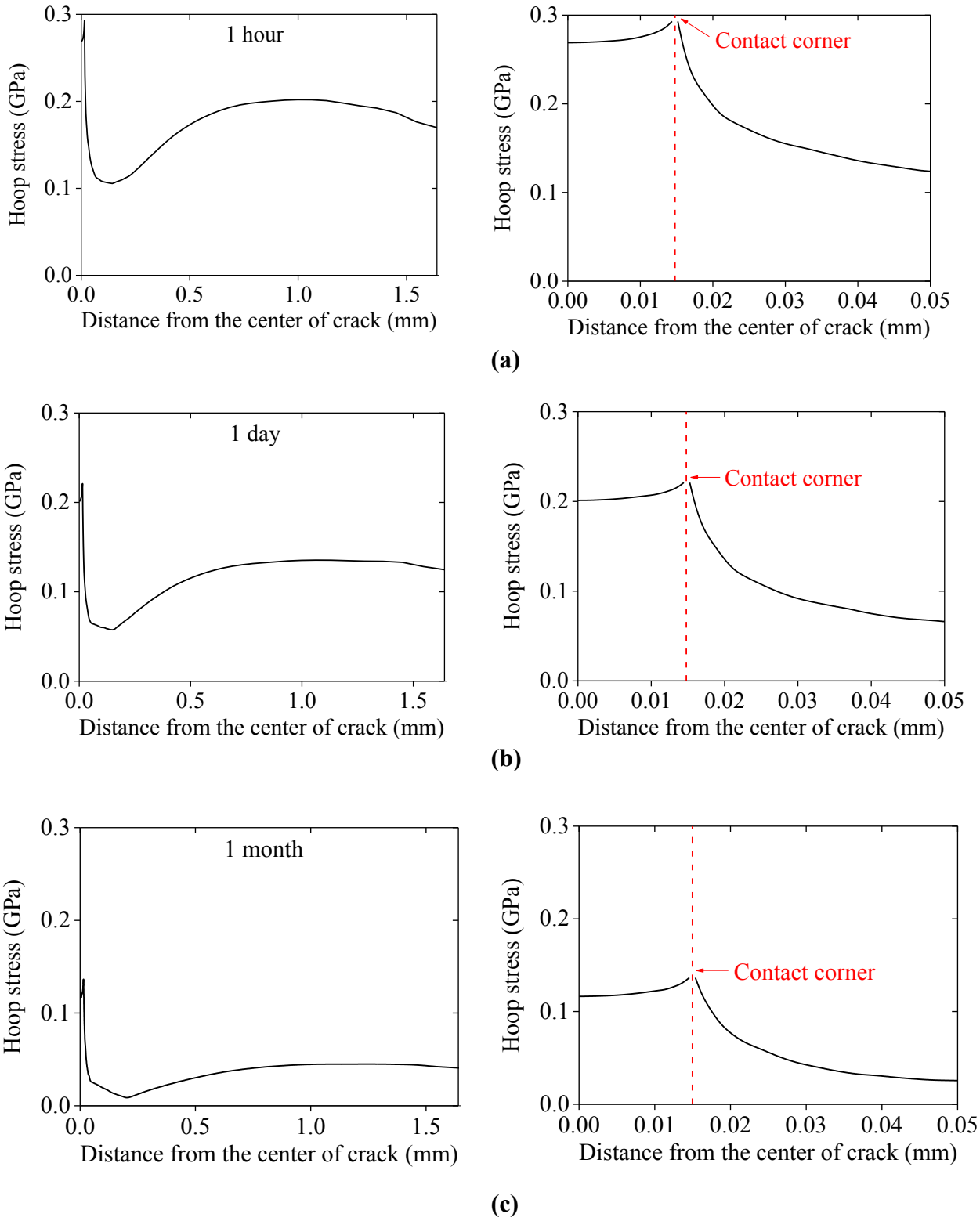

Figure 7: The distribution of hoop stresses at the inner surface of the cladding at **(a)** 1 hour, **(b)** 1 day, and **(c)** 1 month after the onset of a power ramp, with the power history of Fig. 6. The figures on the right show details near the crack mouth.

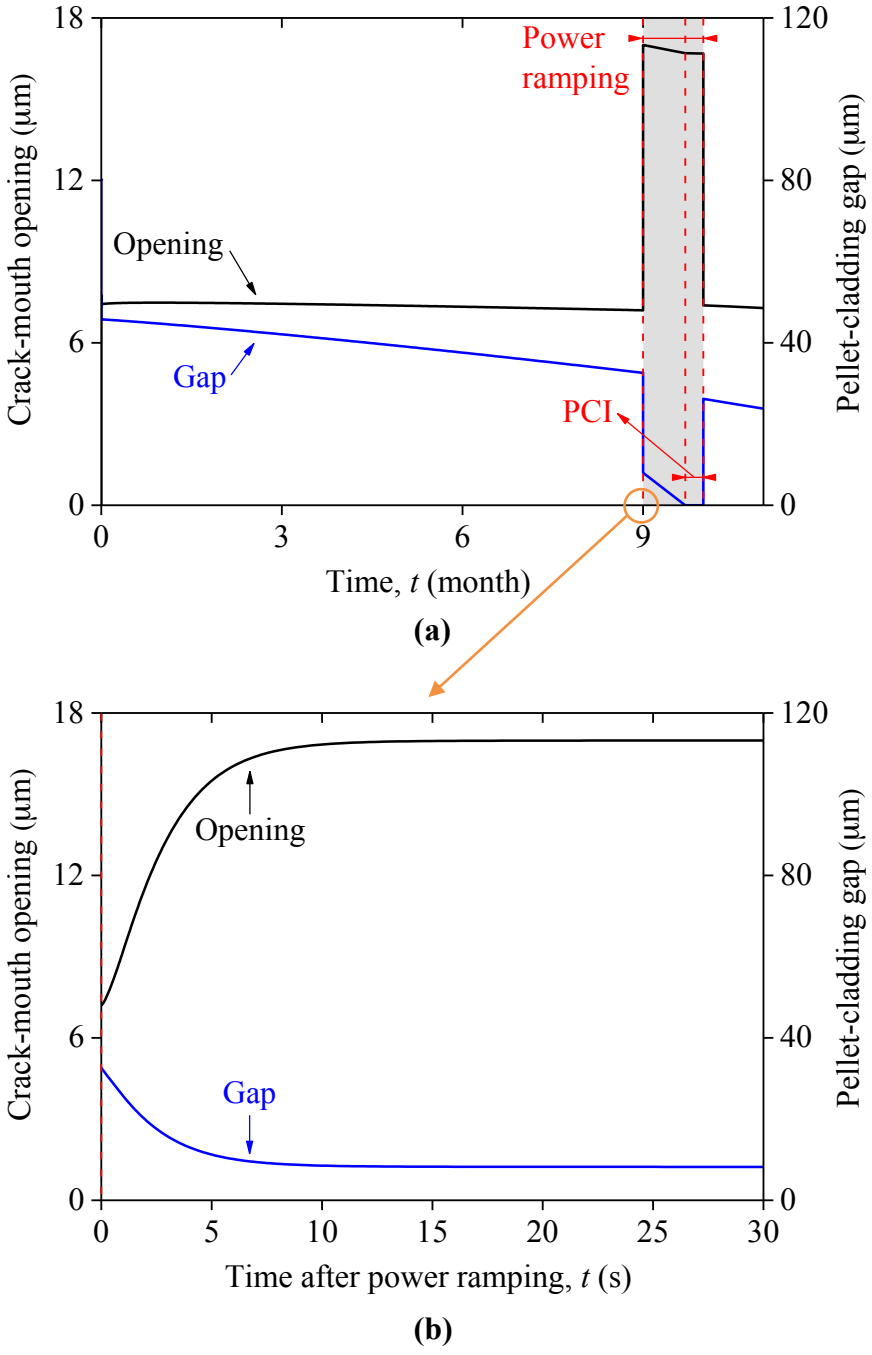

Figure 8: **(a)** The opening of the crack-mouth as a function of time for a cycle consisting of normal operation (LHR = 20 kW/m) for 9 months, a power ramp (LHR = 40 kW/m) for 1 month, and a return to normal operation. The shaded region shows power ramping. **(b)** A plot of crack-mouth opening as a function of time immediately after the beginning of the power ramp.

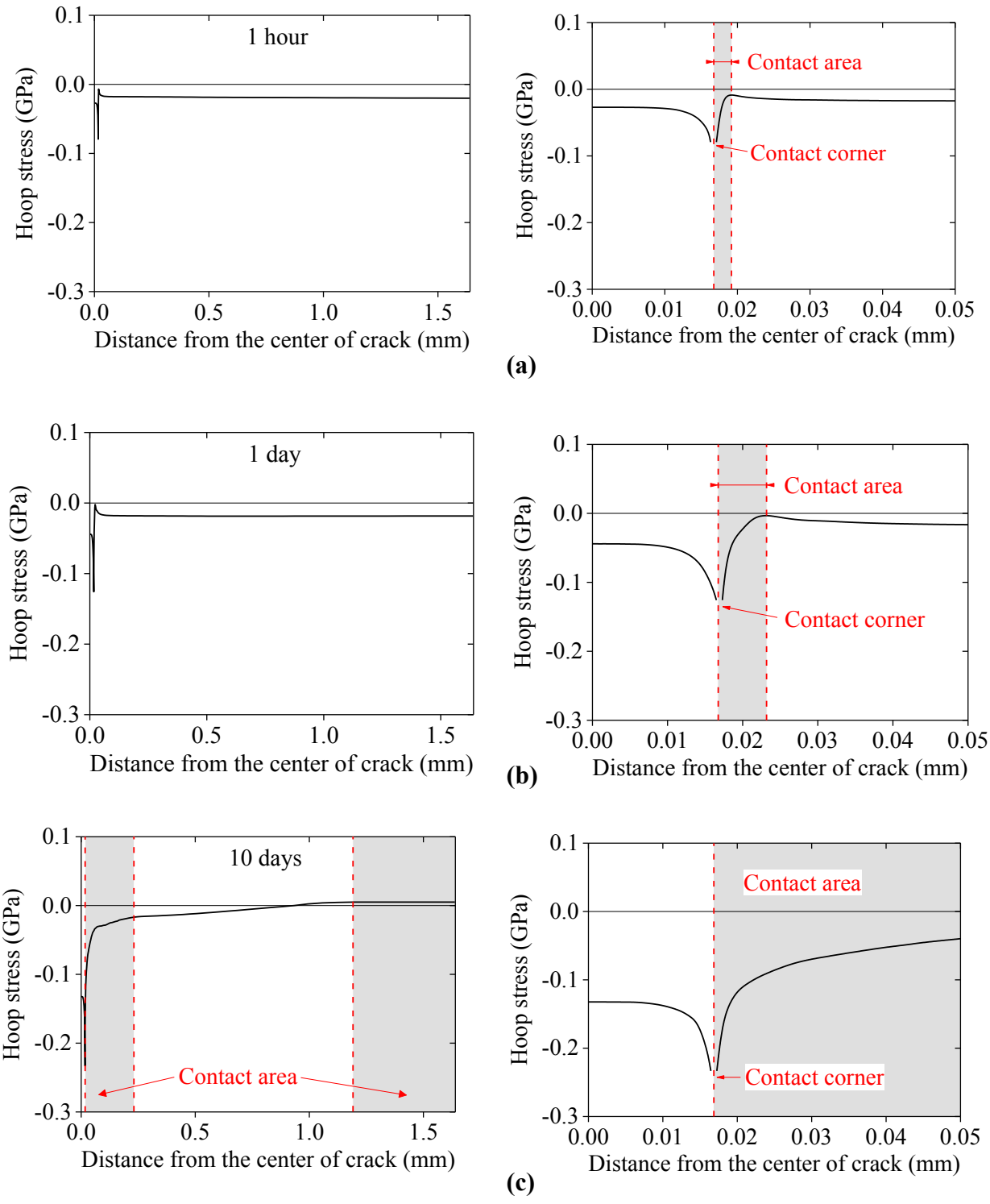

Figure 9: The distribution of hoop stresses at the inner surface of the cladding at **(a)** 1 hour, **(b)** 1 day, and **(c)** 10 days after the onset of a power ramp, with the power history of Fig. 8. The figures on the right show details near the crack mouth.